The American Journal of Pathology, Vol. 181, No. 5, November 2012

http://dx.doi.org/10.1016/j.ajpath.2012.07.019

Immunopathology and Infectious Diseases

Spontaneous Latency in a Rabbit Model of Pulmonary Tuberculosis

Selvakumar Subbian,* Liana Tsenova,*† Paul O'Brien,* Guibin Yang,* Nicole L. Kushner,* Sven Parsons,‡ Blas Peixoto,* Dorothy Fallows,* and Gilla Kaplan*

From the Laboratory of Mycobacterial Immunity and Pathogenesis, The Public Health Research Institute Center at the University of Medicine and Dentistry of New Jersey, Newark, New Jersey; the Biological Sciences Department,† New York City College of Technology, Brooklyn, New York; and the Division of Molecular Biology and Human Genetics,‡ University of Stellenbosch, Tygerberg, South Africa*

Mycobacterium tuberculosis **(Mtb), the causative agent of tuberculosis (TB), is an exquisitely adapted human pathogen capable of surviving for decades in the lungs of immune-competent individuals in the absence of disease. The World Health Organization estimates that 2 billion people have latent TB infection (LTBI), defined by a positive immunological response to Mtb antigens, with no clinical signs of disease. A better understanding of host and pathogen determinants of LTBI and subsequent reactivation would benefit TB control efforts. Animal models of LTBI have been hampered generally by an inability to achieve complete bacillary clearance. Herein, we have characterized a rabbit model of LTBI in which, similar to most humans, complete clearance of pulmonary Mtb infection and pathological characteristics occurs spontaneously. The evidence that Mtb-CDC1551–infected rabbits achieve LTBI, rather than sterilization, is based on the ability of the bacilli to be reactivated after immune suppression. These rabbits showed early activation of T cells and macrophages and an early peak in the *TNFα* level, which decreased in association with clearance of bacilli from the lungs. In the absence of sustained tumor necrosis factor-α production, no necrosis was seen in the evolving lung granulomas. In addition, bacillary control was associated with down-regulation of several metalloprotease genes and an absence of lung fibrosis. This model will be used to characterize molecular markers of protective immunity and reactivation.** ***(Am J Pathol 2012, 181: 1711–1724; http://dx.doi.org/10.1016/j.ajpath.2012.07.019)***

Tuberculosis (TB) has been declared a global public health emergency, accounting for 8.8 million new cases and 1.1 million deaths among HIV-negative people in 2010.[1] In addition to those with known active disease, the World Health Organization has estimated that >2 billion people are latently infected with the causative agent, *Mycobacterium tuberculosis* (Mtb).[2] Individuals with latent TB infection (LTBI) can experience reactivation, leading to active infectious TB later in life, and, thus, pose a huge reservoir of potential new TB cases and additional sources of Mtb infection. These estimates are based on immunological tests, in which LTBI is defined as T-cell recognition of Mtb antigens, determined by either a skin test reaction to Mtb purified protein derivative (PPD) or an *in vitro* interferon gamma blood assay, in the absence of any clinical signs of disease. However, it is not clear whether all individuals diagnosed as having LTBI actually harbor viable Mtb.[3] Autopsy studies have confirmed the presence of viable bacilli in the tissues of individuals who died of other causes, with no known history of TB, but these reports are limited.[4–6] Although individuals with LTBI have only a 5% to 10% lifetime risk of reactivating the infection, the odds are significantly higher with immune compromise, such as that due to HIV infection, diabetes mellitus, or treatment with immune-suppressive drugs. Unfortunately, we presently have no means of identifying which individuals are at greatest risk of reactivating infection. TB control efforts would benefit from a better understanding of the driving forces leading to establishment and maintenance of latency and an ability to predict which individuals are more likely to reactivate LTBI. Recent studies suggest that LTBI is not a single manifestation. Rather, they suggest that TB exists as a spectrum of disease, ranging from the most severe disseminated forms of disease to classic pulmonary

Supported by a grant from the NIH/National Institute of Allergy and Infectious Diseases (RO1 54338 to G.K.).

Accepted for publication July 9, 2012.

Supplemental material for this article can be found at http://ajp.amjpathol.org or at http://dx.doi.org/10.1016/j.ajpath.2012.07.019.

Address reprint requests to Gilla Kaplan, Ph.D., The Public Health Research Institute Center at the University of Medicine and Dentistry of New Jersey, 225 Warren St, Newark, NJ 07103. E-mail: kaplangi@umdnj.edu.

TB, then to subclinical active infection, and, finally, to true LTBI, in which there are no clinical signs of active infection or disease.[5–7]

The outcome of Mtb pulmonary infection is determined by both host and pathogen factors. In addition to host immune compromise, several studies have implicated various genetic polymorphisms in association with resistance or susceptibility to TB in humans.[8–11] On the pathogen side, numerous studies have demonstrated reproducible differences in virulence and/or immunogenicity induced by different clinical Mtb strains.[12–14] Although some studies have compared the host response with large collections of clinical strains, other investigators have taken a more focused approach, using a limited number of strains for more in-depth comparative studies. For example, clinical Mtb strain CDC1551 elicits an early and robust host immune response in mice and in human monocytes, compared with the laboratory strain H37Rv and the clinical strain HN878, a member of the W-Beijing lineage.[15,16] Mtb strain-specific differences in virulence and immunogenicity have been particularly strikingly demonstrated in the rabbit TB infection model.[17–19] By using a rabbit model of TB meningitis, we showed that Mtb CDC1551 infection is more effectively controlled, resulting in lower bacterial colony-forming units (CFUs) in the cerebrospinal fluid and brain, with minimal dissemination to other organs, compared with infection by Mtb HN878, which causes severe pathological characteristics and more dissemination.[20] Similarly, we and others have shown significant Mtb strain-specific differences in the ability of rabbits to control bacillary growth and pathological characteristics after pulmonary infection. In general, although Mtb CDC1551 infection appears to be relatively well controlled, the rabbit is more permissive for growth and dissemination of Mtb HN878; Mtb H37Rv infection produces an intermediate response.[17,18,21]

Several animal models, including mice, guinea pigs, rats, rabbits, and nonhuman primates, have been used to study host and bacterial factors that contribute to the establishment and maintenance of LTBI and reactivation.[22–24] However, none of the published reports from these models has demonstrated reproducible and complete clearance of culturable bacilli from host tissues. Even in the nonhuman primate model, considered the closest to human TB, although approximately 50% of Mtb-infected animals spontaneously develop LTBI, as defined by clinical criteria, it is not possible to predict which animals will control the infection. In addition, subsets of the animals that are defined clinically as latently infected retain many cultivable Mtb in their lungs, lymph nodes, or other tissues.[25,26] This distinction is important because, in most reports of human autopsy studies, Mtb was not directly cultivable from the lungs, but it had to be identified by either an ability to cause disease in guinea pigs or PCR determination of Mtb DNA.[27]

Herein, we have used aerosol infection of rabbits with Mtb CDC1551 to determine whether spontaneous LTBI with complete clearance of cultivable bacilli in the lungs can be established and to evaluate lymphocyte activation and lung pathogenesis during the infection. Furthermore, we have immune suppressed infected rabbits by treatment with corticosteroid to ascertain that the absence of cultivable Mtb in the lungs was not sterilization, but true LTBI.

Materials and Methods

Bacteria and Chemicals

The Mtb CDC1551 strain was obtained from Dr. Thomas Shinnick at the Centers for Disease Control and Prevention (CDC), Atlanta, GA. The bacterial inoculum for infection was prepared by growing the bacilli in Middlebrook 7H9 medium with 10% oleic acid albumin dextrose catalase enrichment (Difco BD, Franklin Lakes, NJ). Stock cultures were banked frozen at −80°C and thawed just before use, as previously described.[28] All chemicals were obtained from Sigma-Aldrich (St Louis, MO), unless otherwise mentioned.

Rabbit Infection and Treatment

Specific pathogen-free, female, New Zealand white rabbits (*Oryctolagus cuniculus*), weighing 2.2 to 2.6 kg, were used ($n = 91$) for aerosol infection by Mtb CDC1551 in four separate experiments ($n = 2$ to 4 per time point per experiment), as previously described.[29] Briefly, rabbits were exposed to Mtb-containing aerosol using a nose-only delivery system. At 3 hours after exposure, a group ($n = 4$) of rabbits was euthanized, and serial dilutions of the lung homogenates were cultured on Middlebrook 7H11 (Difco BD, Franklin Lakes, NJ) agar plates to enumerate the number of initial (time = 0) bacterial CFUs implanted in the lungs. At 2, 4, 8, 12, 20, 24, and 26 weeks after infection (p.i.), groups of rabbits ($n = 2$ to 4) were euthanized and lung, liver, and spleen tissues were harvested for CFU assay, histological analysis, single-cell suspension, and total RNA isolation. Approximately 25% (by weight) of the entire lung, 5% of the liver (in grams), and approximately 50% of the spleen were sampled randomly from different areas of each organ to prepare homogenates for the CFU assay. Undiluted and serially diluted homogenates were placed on Middlebrook 7H11 medium supplemented with 10% oleic acid albumin dextrose catalase enrichment (Difco BD). Starting at 20 weeks p.i., a group of infected rabbits was treated by i.m. injection with triamcinolone at 16 mg/kg body weight daily for 5 days per week for 4 weeks, followed by resting for 2 additional weeks. At 24 and 26 weeks p.i., triamcinolone-treated and triamcinolone-untreated rabbits ($n = 2$ to 3) were euthanized; tissue samples were prepared as previously described. Lung tissues for RNA isolation were snap frozen at −80°C immediately after removal. All animal procedures, including Mtb infection, p.i. housing, necropsy, and processing of infected tissues, were performed in biosafety level 3 facilities, per the approved procedures by the Institutional Animal Care and Use Committee of the University of Medicine and Dentistry of New Jersey, Newark. The animals were fed with food and water ad libitum.

Histological Staining

Portions of lung tissue from Mtb-infected and triamcinolone-treated or triamcinolone-untreated rabbits were fixed in 10% formalin solution, paraffin embedded, and cut into sections (5 μm thick) for staining with H&E to visualize the organization and distribution of leukocytes. One-step trichrome (Gomori) staining was performed on sections to visualize collagen and elastin fibers, as previously reported.[29] The stained sections were analyzed using a Nikon DXM 1200C microscope and photographed at $\times$10 or $\times$40 magnification using NIS-Elements F3.0 software (Nikon Instruments Inc., Melville, NY).

Flow Cytometry Analysis

Single-cell suspensions from Mtb CDC1551-infected rabbit lungs and spleens were prepared and used in flow cytometry analysis, as previously described.[30] Briefly, lung and spleen slices were minced and lung homogenates were digested with collagenase treatment. After incubation with DNase I, the homogenates were passed through a strainer to collect the cells. The erythrocytes were removed by ACK lysis solution (erythrocyte lysing buffer) treatment. The cells were washed thoroughly and stained with trypan blue to determine the viability before use in functional assays. For flow cytometric analysis, purified rabbit lung cells were stained with fluorescein isothiocyanate–conjugated anti-rabbit CD4, phosphatidylethanolamine-conjugated anti-rabbit CD8, or fluorescein isothiocyanate–conjugated anti-rabbit IgG (AbD Serotec Inc., Raleigh, NC) and biotinylated anti-rabbit IgM antibodies (BD Pharmingen, San Diego, CA), followed by avidin-phosphatidylethanolamine for surface staining. The staining for $CD14^+$ cells and for intracellular tumor necrosis factor (TNF)-α was performed with Alexa 647–conjugated anti-human CD14, followed by incubation with biotinylated anti-human TNF-α and avidin-phosphatidylethanolamine. The labeled cells were analyzed using a BD FACS Calibur flow cytometer (BD Biosciences, San Jose, CA) and FlowJo software (Tree Star, Ashland, OR). For the T-cell proliferation assay, purified rabbit spleen cells were stained with carboxyfluorescein succinimidyl ester dye (CFSE), per the manufacturer's guidelines (Life Technologies, Grand Island, NY), and stimulated with either heat-killed and sonicated Mtb CDC1551 or PPD (Staten Serum Institute, Copenhagen, Denmark) or left unstimulated. The cells were stained with either anti-rabbit CD4 or CD8 monoclonal antibodies (BD Biosciences), followed by allophycocyanin-conjugated anti-mouse IgG. The stained cells were acquired using a BD FACS Calibur flow cytometer (BD Biosciences), and the data were analyzed with FlowJo software (Tree Star).

Measurement of Serum Anti-PPD IgG

The amount of circulating IgG in the serum of Mtb CDC1551-infected rabbits was determined as previously reported.[30] Briefly, 96-well plates (Corning Inc., Corning, NY) were coated with PPD and incubated with rabbit serum, followed by primary rabbit anti-PPD polyclonal antibody (Antibodies-Online GmbH, Atlanta). After thorough washings, the wells were incubated with alkaline phosphate–conjugated goat anti-rabbit IgG secondary antibody (Southern Biotech, Birmingham, AL). The alkaline phosphate activity was measured by using Sigma Fast solution, per the instructions of the manufacturer (Sigma-Aldrich, St. Louis, MO). The actual serum IgG amounts were derived from the reference standard of known concentration, run in parallel with the test samples.

Rabbit Lung Total RNA Isolation

Total host RNA from the lungs of Mtb-infected rabbits (n = 3) and matched uninfected control animals (n = 5) at various time points (3 hours and 2, 4, 8, and 12 weeks p.i.) was isolated, as previously described.[31] Briefly, portions of frozen lung tissue were thawed in the presence of 10$\times$ volume (w/v) of TRIzol reagent (Life Technologies) and homogenized on ice. The homogenate was extracted with 0.3 volumes (v/v) of chloroform, and the aqueous phase, containing RNA, was passed through mini spin columns from the NucleoSpin RNA II kit (Macherey-Nagel, Duran, Germany). On-column digestion of the contaminating DNA using DNase I, followed by purification, was performed, as described by the manufacturer. The quality and quantity of the purified RNA were assessed by formaldehyde–agarose gel electrophoresis and a NanoDrop instrument (NanoDrop Products, Wilmington, DE), as previously described.[32]

Microarray Analysis of Rabbit Gene Expression

Total RNA extracted from uninfected and Mtb CDC1551-infected rabbit lungs at 3 hours and 2, 4, 8, and 12 weeks p.i. was used for the microarray experiments, as previously described.[31] Total RNA from individual, Mtb-infected animals was processed separately, and RNA samples from uninfected animals were pooled for microarray analysis. Rabbit whole genome microarray slide and reagents were obtained from Agilent Technologies, Inc. (Santa Clara, CA), and used per the recommendations of the manufacturer. Briefly, total lung RNA from uninfected and Mtb CDC1551-infected rabbits was reverse transcribed and labeled with Cy3 (uninfected) or Cy5 (Mtb-infected) dyes, respectively. The dye incorporation and bias during labeling of cDNA was assessed by a NanoDrop instrument (NanoDrop Products). Equimolar amounts of Cy3- and Cy5-labeled cDNA were mixed and hybridized to the rabbit microarray slides. The slides were processed and spots were scanned, and the Cy3 and Cy5 intensity data were acquired after adjustment for background signals using Agilent Feature Extraction software (Agilent Technologies, Inc.), as previously described.[31] Three microarrays were used for each of the experimental time points using separate RNA samples from two to three animals at 3 hours and 2, 4, 8, and 12 weeks p.i. The extracted raw microarray data were subjected to further statistical analysis using Partek Genomics Suite software, version 6.5 (Partek

Table 1. Description of Target Genes and Oligonucleotide Primers Used in this Study

Gene	Primer	Sequence	Description	Gene ID
TLR2	Forward	5′-CTCTCGCAGAACTTCGTCAA-3′	Toll-like receptor-2	100009578
	Reverse	5′-AGAATGGCGGCGTCGTTGTT-3′		
TNFα	Forward	5′-CTGAGTGACGAGCCTCTAGC-3′	TNF-α	100009088
	Reverse	5′-TTCATGCCGTTGGCCAGCAG-3′		
CD14	Forward	5′-GCTATGCTGACGTAGTCAAG-3′	Monocyte differentiation antigen	100008983
	Reverse	5′-GGTGCCAGTTACCTCTATGT-3′		
CAV1	Forward	5′-GCGACCCCAAGCATCTCA-3′	Caveolin 1	100008837
	Reverse	5′-GATGGTAGACAGTAGGCG-3′		
NP4	Forward	5′-TGGACGTGGCCGTCTACATT-3′	Microbicidal peptide-beutrophil proteinase-4	100009135
	Reverse	5′-TGTGGCGGACTCCATTGACT-3′		
VCAM1	Forward	5′-CTGGAGGATGCAGGAGTGTA-3′	Vascular cell adhesion molecule-1	100008901
	Reverse	5′-GAGCACGAGAAGTTCAGG-3′		
LGALS3	Forward	5′-AGGGAAGAAAGGCAGACGAC-3′	Galactose- binding lectin, 3	100009187
	Reverse	5′-CATCATTGACCGCAACCTTG-3′		
PRKC	Forward	5′-CCATCGGTCTGTTCTTCCTA-3′	Protein kinase C	100037719
	Reverse	5′-GTCAGCGATCTTGATGTGTC-3′		
MMP9	Forward	5′-CGCCAGCTACGACAAGGACA-3′	MMP-9	NM_001082203.1
	Reverse	5′-AAGTGGTGGCACACCAGAGG-3′		
MMP12	Forward	5′-CCAACTGGCTGTGACCACAA-3′	MMP-12	NM_001082771.1
	Reverse	5′-AGCAGCCTCAATGCCTGAAG-3′		
MMP14	Forward	5′-CCACAAGATGCCTCCTCAAC-3′	MMP-14	NM_001082793.1
	Reverse	5′-GTAGCCGTCCATCACTTGGT-3′		
TIMP1	Forward	5′-AGACGGCCTTCTGCAACTCC-3′	Tissue inhibitor of metalloproteinase-1	100009047
	Reverse	5′-AACTCCTCGCTGCGGTTCTG-3′		
GAPDH	Forward	5′-GGCGTGAACCACGAGAAGTA-3′	Glyceraldehyde 3-phosphase dehydrogenase	100009074
	Reverse	5′-TCCACAATGCCGAAGTGGTC-3′		

MMP, matrix metalloproteinases.

Inc., St. Louis, MO). To determine the statistically differentially expressed genes, we used *P* value of significance from two-way analysis of variance. $P \leq 0.05$ was considered statistically significant. We previously showed that selection of genes using *P* values, rather than arbitrary expression level as cutoff values, enriches for genes that are functionally more significant.[30] The microarray data have been submitted to Gene Express Omnibus (*http://www.ncbi.nlm.nih.gov/geo;* accession number GSE39219).

Pathway Analysis of Differentially Expressed Rabbit Genes

The differentially expressed rabbit genes that are statistically significant ($P \leq 0.05$) and annotated were uploaded to Ingenuity Pathway Analysis (IPA) software (Ingenuity Systems, Redwood City, CA) for further analysis, as previously reported.[31] Because the IPA knowledge base does not have rabbit gene information, we used the cumulative functional orthologous data from human, mouse, and rat genomes for the pathway analysis and network derivation. In IPA, the significance of a functional pathway/network composed of differentially expressed genes is determined by the *P* value calculated using the right-tailed Fisher's exact test.

Real-Time qPCR Analysis

Total RNA from uninfected and Mtb-infected rabbit lungs at 3 hours and 2, 4, 8, and 12 weeks p.i. was reverse transcribed into cDNA using the AffinityScript QPCR cDNA Synthesis Kit, following the instructions of the manufacturer (Agilent Technologies, Inc.). The quantitative (q)PCR experiments were performed on a Stratagene Mx3005p machine (Agilent Technologies, Inc.) with cDNA and site-specific oligonucleotide primers of target genes, using Brilliant III Ultra-Fast SYBR Green QPCR Master Mix, according to the product instructions (Agilent Technologies, Inc.). The inert, passive reference dye, ROX, was added to all of the test samples. No SYBR Green and no cDNA control samples were included in one of the triplicate assays for each experimental time point. The housekeeping gene, *GAPDH*, was included to normalize the levels of expression of test samples. The amplicon sizes of *GAPDH* and test genes were between 90 and 250 bp. The C_T value was determined using MxPro4000 software (Agilent Technologies, Inc.) after setting uniform baseline fluorescence for all of the samples in each experiment. The fold change in gene expression was calculated from the formula, $2^{-\Delta\Delta C}{}_T$, in which ΔC_T is the difference in C_T between the test gene and *GAPDH*. Each experiment was repeated at least three times with cDNA from two to four animals per experimental time point per group. Table 1 contains a description of the tested genes, their accession numbers, and the DNA sequence of primers used in the qPCR experiments.

Statistical Analysis

The rabbit microarray data were analyzed by analysis of variance using Partek Genomics Suite software, version 6.5 (Partek Inc.), and the significance of the functional pathway/network was determined by Fisher's exact test using IPA (Ingenuity Systems). An independent Student's *t*-test from GraphPad Prism software, version 5.02

(GraphPad Software, La Jolla, CA), was used for the analysis of flow cytometry and qPCR data, and the mean ± SD or median ± SE values, respectively, were plotted. For all of the experiments, $P \leq 0.05$ was considered statistically significant.

Results

Growth of Mtb CDC1551 in Infected Rabbits

After infection of rabbits with Mtb CDC1551, the growth kinetics were evaluated by measuring the number of CFUs in various organs of the rabbits. In the lungs, Mtb CDC1551 grew exponentially from 3.5 $\log_{10}$ at exposure (time = 3 hours) to approximately 5 $\log_{10}$ at 4 weeks p.i. Thereafter, the numbers of CFUs declined gradually. By 12 weeks, no cultivable bacteria were found in the lungs of some of the rabbits (approximately 30%), whereas the others still had detectable CFUs (Figure 1, A and B). By 20 weeks, all rabbits had no detectable CFUs in the lungs. No CFUs were found in the livers or spleens of the infected rabbits at any of the tested time points (data not shown). This pattern of active bacillary growth up to 4 weeks, followed by a gradual reduction in CFUs and complete clearance of cultivable bacilli from the lungs, was similar for a range of initial bacillary loads. However, the time to complete clearance of the CFUs differed, depending on the exact infectious dose, so that a higher initial bacillary load took a longer time to clear. After infection with 4 $\log_{10}$, approximately 30% of rabbits cleared the infection by 20 weeks, and all cleared the infection by 24 weeks, p.i. (Figure 1B). More important, bacillary clearance was not the result of sterilization of the infection, as demonstrated by our ability to reactivate the infection by immune suppression of rabbits at 20 weeks p.i. Four weeks of treatment with the corticosteroid, triamcinolone, resulted in resumed bacterial growth and a consistent increase in CFUs in the lungs. At the end of triamcinolone treatment (24 weeks), approximately 4.7 $\log_{10}$ CFUs were measured in the lungs; the bacillary load remained stable (from 24 to 26 weeks) after the drug treatment was discontinued (Figure 1A). At 24 and 26 weeks p.i., 8 of 8 and 8 of 9 rabbits, respectively, had no detectable CFUs in the lungs. Thus, among the rabbits infected for >20 weeks, spontaneous reactivation or persistence was seen in only 1 of 17 infected rabbits (described later).

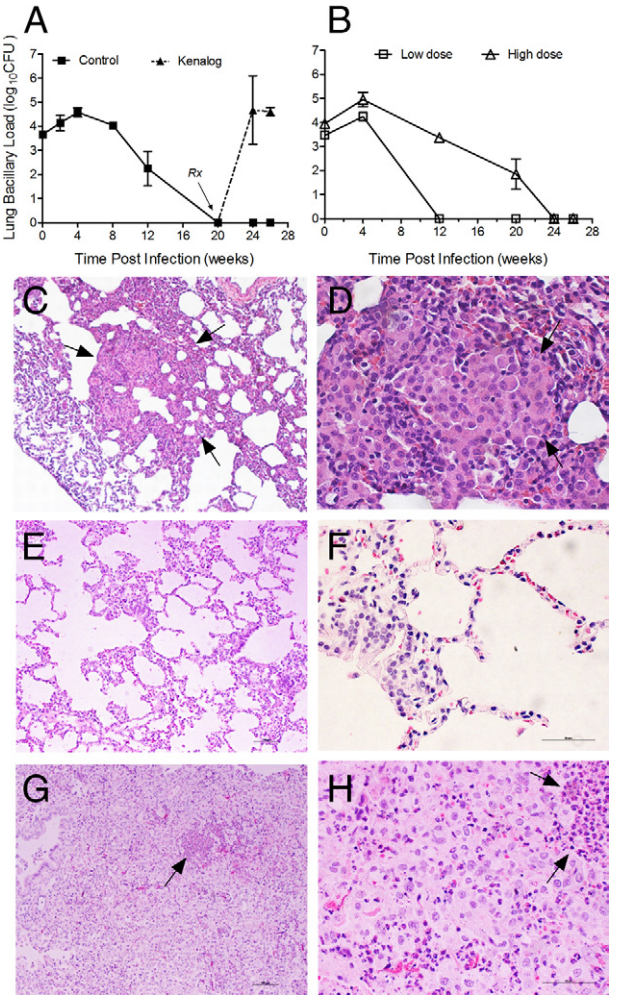

Figure 1. Lung bacillary load and histopathological characteristics during *Mtb* CDC1551 infection of rabbits. **A:** Kinetics of Mtb growth in the infected lungs of untreated and triamcinolone (immune suppression) treated rabbits. Complete clearance of cultivable bacilli is noted at 20 weeks p.i.; 4 weeks of triamcinolone treatment (**arrow**) resumed bacillary growth in the infected rabbit lungs. **B:** Kinetics of bacillary growth and clearance in the lungs of rabbits infected with a low or high dose of Mtb CDC1551. No bacterial CFUs are obtained in the rabbit lungs after 12 or 24 weeks in the low- and high-dose infections, respectively. Values are given as mean ± SD, obtained from 91 rabbits in four separate experiments, with four to five animals per time point (**A** and **B**). **C–H:** Histopathological characteristics of rabbit lungs infected with Mtb CDC1551. **C** and **D:** Lungs of infected, untreated rabbits at 8 weeks p.i., showing well-organized granulomas containing aggregates of mononuclear cells (**arrows**) surrounded by a lymphocytic cuff. **E** and **F:** Mtb CDC1551-infected rabbit lungs at 24 weeks p.i., without triamcinolone treatment. In both **E** and **F**, almost normal lung parenchyma and alveoli with moderately elevated cellularity can be seen. **G** and **H:** Histological characteristics of Mtb-infected rabbit lungs, treated with triamcinolone for 4 weeks, initiated at 20 weeks p.i. Large suppurative infiltration with many macrophages and polymorphonuclear leukocytes (**arrows**) that contain red granules in their cytoplasm are seen. Scale bars: 100 μm (**C**, **E**, and **G**); 50 μm (**D**, **F**, and **H**). All sections were stained with H&E and photographed. Original magnification: ×10 (**C**, **E**, and **G**); ×40 (**D**, **F**, and **H**).

Pathological and Histopathological Characteristics in Mtb CDC1551-Infected Rabbit Lungs

Examination findings of the lungs of Mtb CDC1551-infected rabbits showed no macroscopic lesions from 2 to 12 weeks p.i. (see Supplemental Figure S1 at *http://ajp.amjpathol.org*). In only 1 of 17 infected animals, a single macroscopic subpleural granuloma was visible at 20 weeks p.i. (described later). In contrast, H&E staining of the lung sections, followed by a histological examination, revealed multiple microscopic lesions in the lungs of all rabbits from 4 to 12 weeks p.i. (Figure 1, C and D; see also Supplemental Figure S1 at *http://ajp.amjpathol.org*). Granulomatous foci, seen at 4 weeks, had small aggregates of macrophages and lymphocytes. Granulomas enlarged into well-organized structures with more cells at 8 weeks. No necrosis or caseation was observed in any

granulomas. At 12 weeks, the granulomas began to resorb, becoming smaller and less cellular (see Supplemental Figure S1 at *http://ajp.amjpathol.org*). By 20 and 24 weeks p.i., the lung parenchyma and alveoli displayed mildly elevated cellularity, with no intact granulomas and minimal signs of tissue damage or fibrosis (Figure 1, E and F; see also Supplemental Figure S1 at *http://ajp.amjpathol.org*). In contrast, the lung sections of infected rabbits treated for 4 weeks with triamcinolone (from 20 to 24 weeks) showed large suppurative diffuse infiltration of immune cells, composed primarily of macrophages and polymorphonuclear leukocytes (Figure 1, G and H). Thus, the histopathological profile correlated with the lung bacterial load. The increase in bacterial CFUs, followed by a gradual containment of the bacterial growth and complete clearance over time, was associated with an initial cellular response, followed by resolution of lung pathological characteristics as the CFUs declined. The increased bacterial CFUs seen in the infected rabbits on immune suppression–induced reactivation was accompanied by renewed recruitment of leukocytes into the lungs.

Interestingly, as previously mentioned, at 20 weeks p.i., 1 of 17 Mtb CDC1551-infected rabbits had a single, visible, subpleural unresolved lesion in the right lower lobe of the lungs (Figure 2A). The results of a histological examination of this lesion showed a large cellular granuloma with a central area of epithelioid macrophages surrounded by a prominent lymphocytic cuff (Figure 2, B and C). When cultured for bacteria, the lesion contained a bacillary load of approximately 2.8 $\log_{10}$ CFUs (see Supplemental Table S1 at *http://ajp.amjpathol.org*). In contrast, other areas of the lung of this rabbit (seven different samples) had no detectable CFUs and no visible granulomas. Similarly, in one rabbit infected for 26 weeks, residual infection (Mtb CFU) was found in one focused area in the right lung, which was not evaluated for pathological characteristics (data not shown).

Mononuclear Cellular Composition in the Mtb CDC1551-Infected Rabbit Lungs

The distributions of mononuclear leukocyte populations in single-cell suspensions prepared from infected rabbit lungs ($n = 4$ to 5 per time point) were determined by flow cytometry (Table 2). Of the total mononuclear cell population isolated from the infected rabbit lungs, an increase in the percentage of nonlymphocyte mononuclear cells was observed from 4 to 8 weeks, which was maintained at similar levels at 12 weeks. Among the total lymphocyte populations, the percentages of $CD4^+$ and $CD8^+$ cells were relatively low at 4 weeks and peaked at 8 weeks p.i. (Table 2). A strikingly high percentage of the total lymphocyte population was B cells (>70%). However, the anti-IgG antibodies used to identify B cells may have also bound to Fc receptors expressed on the surface of other cell types, leading to an overestimation of this cell population. Since anti-IgG staining was not seen in the macrophages, which express high levels of Fc receptors, but only in the lymphocyte population, it was likely that the

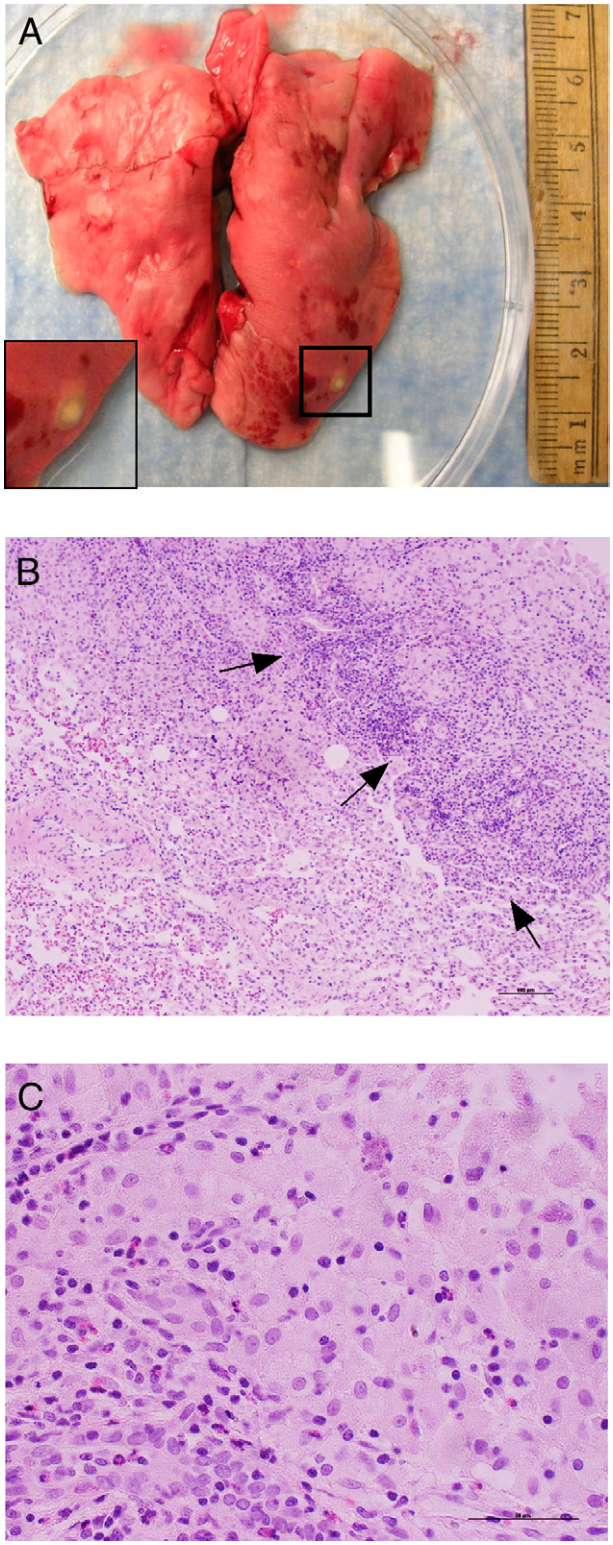

Figure 2. Gross pathological and histological characteristics of Mtb CDC1551-infected rabbit lung harboring a persistent or spontaneously reactivated (percolator) granuloma at 20 weeks of infection. **A:** A single subpleural lesion is clearly visible in the bottom right lobe of the lung (box and **inset**) obtained from one of the Mtb-infected rabbits without the immune-suppression treatment. **B** and **C:** Histological staining of the lung with percolator granuloma showing a large, coalescent granulomatous lesion with an area of epithelioid macrophages, surrounded by a lymphocytic cuff (**arrows**). Scale bars: 100 μm (**B**); 50 μm (**C**). The tissue sections were stained with H&E and photographed. Original magnification: ×10 (**B**); ×40 (**C**).

Table 2. Immune Cell Composition in Mtb CDC1551-Infected Rabbit Lungs

Time p.i. (weeks)	Nonlymphocyte mononuclear cells*	Lymphocytes*	$CD4^{+\dagger}$	$CD8^{+\dagger}$	B cells†	Serum IgG‡
4	32.8 ± 4.6	66.7 ± 4.7	3.4 ± 0.5	3.9 ± 2.0	79.3 ± 6.3	2.0 ± 0.8
8	72.2 ± 2.9	27.3 ± 3.0	19.1 ± 1.5	6.1 ± 0.6	73.7 ± 4.0	3.2 ± 0.8
12	64.1 ± 7.4	35.7 ± 7.4	3.4 ± 0.6	2.0 ± 0.5	86.1 ± 2.4	3.0 ± 0.6

Data are given as mean ± SD. The percentages of cells in single-cell suspensions were identified by immunostaining and flow cytometry.
*Data are given as percentage of total mononuclear cell population.
†Data are given as percentage of total lymphocyte gated cell population.
‡IgG levels are expressed as ng/μL on a $\log_{10}$ scale. The IgG value at baseline (3 hours after infection) was 2.0 ± 0.2.

binding was B-cell specific. By using a novel enzyme-linked immunosorbent assay, we measured the anti-PPD-IgG levels in the serum of CDC1551-infected rabbits.[30] Surprisingly, there was only a limited increase in the levels of serum IgG as the infection progressed from 4 to 12 weeks. The increase was not statistically significant compared with the baseline values (3 hours p.i.) (Table 2).

Spleen T-Cell Activation during Mtb CDC1551 Infection

The activation of host T cells was evaluated after infection with Mtb CDC1551 (Figure 3). To enumerate the populations of antigen-specific proliferating $CD4^+$ and $CD8^+$ T cells, single-cell suspensions of the spleen from infected rabbits (n = 4 to 5 per time point) were labeled with CFSE. Cells were stimulated with either PPD or heat-killed sonicated Mtb CDC1551, and the percentages of proliferating T lymphocytes were determined by the dilution of CFSE and compared with the labeled, but unstimulated, cells using flow cytometry (Figure 3). At 4 weeks, the percentage of proliferating $CD4^+$ cells had increased in the PPD (79.5 ± 2.7) and Mtb (78.1 ± 3.2) stimulated and unstimulated (66.5 ± 7.1) cells. The differences between the stimulated and unstimulated groups were not statistically significant. By 8 weeks, the percentage of proliferating $CD4^+$ cells was significantly reduced ($P < 0.05$) in all three stimulation groups (Figure 3, A and B). At this time, significantly more ($P < 0.05$) proliferating $CD4^+$ cells were observed in response to PPD (50.4 ± 0.9) and Mtb (34.5 ± 4.4) stimulation compared with the unstimulated cells (16.3 ± 3.4). PPD induced significantly ($P < 0.001$) more proliferating $CD4^+$ cells compared with Mtb stimulation. At 12 weeks, the percentage of $CD4^+$ cells proliferating in response to PPD (51.7 ± 28.3) and Mtb (52 ± 27.6) stimulation was comparable and significantly higher than the unstimulated (19.9 ± 7.1) cells (Figure 3B). By 20 weeks, the percentage of proliferating $CD4^+$ cells had declined significantly ($P < 0.05$) compared with 12 weeks for both PPD (19.3 ± 2.7) and Mtb (15.2 ± 4.3) stimulation. The percentage of $CD4^+$ cell proliferation further declined significantly by 24 weeks ($P < 0.05$) in the PPD-stimulated group (6.7 ± 1.9) but not in the Mtb-stimulated group (11.5 ± 4.5). The percentage of proliferating unstimulated cells remained similarly low from 8 to 24 weeks of infection.

In contrast to the $CD4^+$ cells, the percentage of proliferating $CD8^+$ cells increased from 4 weeks to reach a maximum at 8 weeks in response to both PPD and Mtb stimulation (Figure 3, C and D). Although there was no significant difference in the percentage of proliferating $CD8^+$ cells among the PPD (70.8 ± 9.6) or Mtb (73 ± 8.9) stimulated and unstimulated (50.7 ± 13.8) cells at 4 weeks, $CD8^+$ cell proliferation was significantly increased ($P < 0.005$) in response to Mtb (87.1 ± 0.8) and PPD (91.6 ± 1) stimulation compared with unstimulated cells (56.7 ± 3.2) at 8 weeks (Figure 3D). At 12 weeks, the percentage of proliferating $CD8^+$ cells in the PPD (63.5 ± 26.5) and Mtb (67.9 ± 23.3) stimulated groups had decreased to the level seen in the unstimulated cells (54.8 ± 23.2). As observed for the $CD4^+$ cells, the percentage of proliferating $CD8^+$ cells was reduced significantly ($P < 0.01$) at 20 and 24 weeks p.i. in the PPD

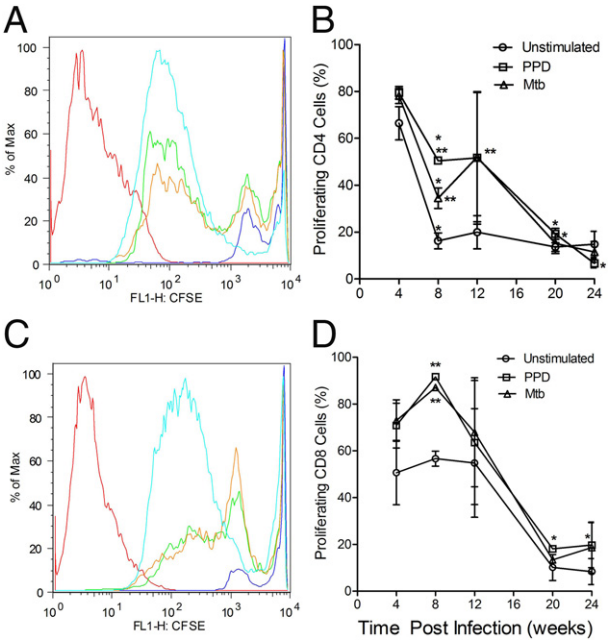

Figure 3. Flow cytometry analysis of spleen T-cell proliferation in Mtb CDC1551-infected rabbits. **A** and **B:** The percentage of proliferating spleen CD4 T cells cultured with PPD or Mtb or unstimulated. In **B**, the statistically significant differences between various stimulants at different time points after infection are denoted by either a **single asterisk** (compared with a previous experimental time point; $P < 0.05$) or a **double asterisk** (compared with unstimulated conditions; $P < 0.05$). **C** and **D:** The percentage of proliferating spleen CD8 T cells cultured with PPD or Mtb or unstimulated. In **D**, the statistically significant differences between various stimulants at different time points after infection are denoted by either a **single asterisk** (compared with 8 weeks p.i.; $P < 0.05$) or a **double asterisk** (compared with unstimulated and PPD- or Mtb-stimulated conditions; $P < 0.05$). The color code in **A** and **C** corresponds to proliferation of cells stimulated with concanavalin A (red), PPD (light blue), or Mtb (green), unstimulated cells (orange), and cells with no CFSE (dark blue). Values plotted in the graph are mean ± SD, measured in samples from at least three animals.

Table 3. Distribution of Activated Macrophages in the Mtb CDC1551-Infected Rabbits

	Lung		Spleen	
Time p.i. (weeks)	$CD14^{+}$*	$CD14^{+}$ TNF-α^{+}†	$CD14^{+}$*	$CD14^{+}$ TNF-α^{+}†
4	38.6 ± 11	10.5 ± 1.4	25.1 ± 11	9.1 ± 2.0
8	58.2 ± 4	38.4 ± 1.1	12.9 ± 1.0	15.5 ± 3.9
12	15.0 ± 2	7.8 ± 1.0	10.0 ± 1.4	6.8 ± 0.2

Data are given as mean ± SD percentages of cells stained in single-cell suspensions.
*Data are given as percentage of total mononuclear cell population.
†Data are given as percentage of total $CD14^{+}$ gated cell population.

(18.1 ± 1 and 19.7 ± 9.6, respectively) or Mtb (13.4 ± 1.2 and 18.6 ± 10.9, respectively) stimulated and unstimulated (10.16 ± 5.5 and 8.4 ± 5.5, respectively) conditions (Figure 3D). Taken together, these results suggested a strong and rapid activation and proliferation of T cells at 4 and/or 8 weeks in the Mtb CDC1551-infected rabbits, which then declined as the antigenic load was reduced.

Macrophage Activation in the Lungs and Spleen during Mtb CDC1551 Infection

To determine the proportion of activated macrophages, single-cell suspensions were prepared from infected rabbit lungs and spleens at 4, 8, and 12 weeks, and the cells were stained for CD14 and intracellular TNF-α. The percentage of $CD14^{+}$ cells and $CD14^{+}$TNF-α^{+} was enumerated by flow cytometry. The percentage of $CD14^{+}$ cells in the lungs increased from 4 weeks (38.6%) to 8 weeks (58.2%) and then declined at 12 weeks p.i. (15%). In the spleen, $CD14^{+}$ cell populations were relatively high at 4 weeks (25.1%), then declined by 8 weeks (12.9%), and stabilized at comparable levels up to 12 weeks p.i. (Table 3). The percentage of $CD14^{+}$ cells that expressed TNF-α increased in the lungs from 10.5% to 38.4% between 4 and 8 weeks and declined to 7.8% at 12 weeks p.i. Similarly, in the spleen, the percentage of $CD14^{+}$TNF-α^{+} cells increased significantly from 9.1% at 4 weeks to 15.5% at 8 weeks, followed by a decline at 12 weeks (6.8%) (Table 3). Thus, in the Mtb CDC1551-infected rabbits, peak macrophage activation, as determined by intracellular TNF-α staining, occurred at 8 weeks in both the lungs and the spleen and declined as the bacillary load was reduced.

Transcriptional Analysis of Selected Cellular Pathway Genes in Rabbit Lungs during Mtb CDC1551 Infection

Because both the granulomatous response and macrophage activation in the lungs of CDC1551-infected rabbits peaked and then declined as the bacillary load was cleared, we examined whether inflammation and fibrosis/tissue remodeling followed a similar pattern of expression in infected rabbit lungs. Whole genome microarray was used to analyze the transcription profile of selected networks associated with pathogenesis induced in Mtb CDC1551-infected rabbit lungs at 2, 4, 8, and 12 weeks p.i. and compared with the expression levels in uninfected animals. The microarray data have been submitted to Gene Express Omnibus (accession number GSE39219). Significantly differentially expressed genes were selected based on $P \leq 0.05$ and used in selected pathway analysis and network derivation. The transcript level of genes involved in inflammation and fibrosis/tissue modeling networks was used for network construction using IPA software (Figure 4). Of the 25 genes in the inflammation network, 21 were significantly differentially expressed at 2 weeks compared with uninfected lungs (8 were increased, and 13 were decreased) (Figure 4, A and B). The number of up-regulated genes decreased at 4, 8, and 12 weeks to six, five, and two genes, respectively. In addition, the number of down-regulated genes increased from 13 at 2 weeks to 16, 18, and 15 at 4, 8, and 12 weeks, respectively. In addition to *TNF*α, expression of *NR3C1*, *HLA-C*, *TLR2*, *HPX*, *NOS2*, *SLC10A2*, and *FTL* were significantly up-regulated at 2 weeks, whereas genes encoding cytokines/chemokines (*IL15*, *CSF2*, *IL1B*, *CCL2*, and *IL8*), cell surface molecules (*CD1D*, *TNFSF13B*, *TLR3*, and *VCAM1*), enzymes (*ARG2*, *PTGS2*, and *F3*), and a transcriptional regulator (*SMAD4*) were down-regulated at this time. By 12 weeks p.i., only *NR3C1* and *TLR2* remained up-regulated, whereas most of the other genes, including *TNF*α, were significantly down-regulated compared with uninfected lungs. Transcript levels of *CD1D*, *IL15*, *SMAD4*, and *TLR3* were transiently up-regulated from 2 to 4 and/or 8 weeks and then down-regulated again (Figure 4A). Overall, the expression pattern of genes suggested a moderate up-regulation of the inflammation network at 2 weeks, which then declined as the infection and bacterial burden decreased in the lungs.

Of the 25 genes in the tissue fibrosis and remodeling network, the number of significantly up-regulated genes gradually decreased from 2 (14 genes) to 4 (11 genes), to 8 (8 genes), and to 12 (3 genes) weeks p.i. (Figure 4, C and D). In contrast, the number of down-regulated genes increased from 7 (2 weeks) to 10 (4 weeks), to 13 (8 weeks), and to 12 (12 weeks). Only *TIMP1* and *PRKCB* were up-regulated from 2 to 12 weeks, whereas *IFNG*, *TNNT2*, *PLAU*, *VTN*, *ELANE*, and *AHR* expression was sustained from 2 to 4 or 8 weeks and then declined (Figure 4C). *FAS*, *IL4*, and *CAV1* increased transiently and then declined. *MMP14*, *MMP13*, *MMP9*, and *MMP12* were down-regulated to varying degrees at all time points. Taken together, the expression pattern of fibrosis and tissue remodeling network genes suggested a transient activation of this network in the Mtb CDC1551-in-

fected rabbit lungs at 2 weeks, with a decline in activation as the bacilli cleared and the granulomas resorbed.

To validate the microarray results and to analyze the expression of inflammation and fibrosis/tissue remodeling genes in the lungs of infected rabbits, we measured the transcript levels of selected genes at 2, 4, 8, and 12 weeks using real-time quantitative PCR (qPCR) and compared them with corresponding levels in uninfected animals (Figure 5). The list of selected genes involved in these pathways includes *TLR2*, *TNFα*, *CD14*, *CAV1*, *NP4*, *VCAM1*, *LGAL*, *PRKC*, *MMP9*, *MMP12*, *MMP14*, and *TIMP1*. The expression pattern of most of the selected inflammatory genes and all of the fibrosis/tissue remodeling genes was consistent with the microarray results. Compared with uninfected rabbit lungs, the expression of *CD14* was moderately up-regulated at all time points. Transcription of a defensin (*NP4*) was up-regulated >10-fold in the rabbit lungs at 2 weeks, and remained elevated up to 12 weeks. *TNFα* transcript levels were transiently, but significantly, up-regulated at 2 weeks, whereas *VCAM1* was down-regulated from 2 until 12 weeks p.i. Similarly, except for *TIMP1* and *PRKC*, the selected genes in the fibrosis/tissue remodeling network were predominantly down-regulated at all time points (Figure 5). Overall, consistent with the microarray analysis, these results suggested an early transient macrophage activation/inflammation (2 weeks) and complete down-regulation of the tissue fibrosis/remodeling network at later times of infection.

Lung Fibrosis in the Mtb CDC1551-Infected Rabbits

The results from transcriptional analysis suggested that macrophage activation/inflammation and fibrosis/tissue remodeling pathways are transiently activated but not chronically induced in the rabbit lungs in response to Mtb CDC1551 infection. To determine the corresponding alterations in the pathological characteristics during the infection, lung sections were stained by Gomori trichrome and analyzed microscopically for collagen deposition, fibrosis, and tissue remodeling (Figure 6). Despite the formation of a clearly demarcated cellular granuloma, with central areas of macrophages and peripheral lymphocytic cuffs, only moderate compression of the lung tissue surrounding the granuloma was noted at 12 weeks p.i. (Figure 6A). The absence of fibrosis, which is typical of progressive TB, was striking (Figure 6, B and C). The background staining for collagen observed in the lung tissue adjacent to the granulomas (Figure 6C) was similar to that seen in uninvolved areas of the lung (Figure 6, A and B). No significant collagen staining and fibrosis were observed in the lung granulomas at any of the other tested time points (data not shown). This was in stark contrast to the highly fibrotic lesions seen when rabbits were infected for 12 to 16 weeks with Mtb HN878, which led to chronic granulomatous disease rather than latency in the animals.[29]

Discussion

We have characterized a model of LTBI in rabbits in which, similar to 90% of immune-competent humans, complete clearance of pulmonary Mtb infection and pathological characteristics occurs spontaneously. The evidence that Mtb CDC1551-infected rabbits achieved LTBI, rather than sterilization, is based, as in humans, on the ability of the bacilli to be reactivated after immune suppression.[3,33] This model can be used to fully characterize the molecular markers of protective immunity and reactivation. In addition, this model will be useful to study the antibacterial activity of drugs during nonreplicating persistence of Mtb.

After Mtb CDC1551 aerosol infection, we observed early peaks in the proliferative capacity of $CD4^+$ and $CD8^+$ T cells from the spleen (4 or 8 weeks p.i., respectively), which declined rapidly, concurrent with a reduction in the bacillary load in the lungs. Similarly, *IFNγ* expression in the infected lungs showed an early up-regulation from 2 weeks p.i., returning to basal levels by 12 weeks. This pattern is in stark contrast to our observations in Mtb HN878-infected rabbits with chronic granulomatous TB, in which peak spleen $CD4^+$ and $CD8^+$ T-cell proliferative capacity was delayed (8 and 12 weeks, respectively) and then persisted at relatively high levels.[30] Interestingly, the T cells harvested from the spleens of Mtb CDC1551-infected rabbits showed two different phenotypes in *ex vivo* assays: cells proliferating in the absence of exogenously added antigen and cells proliferating in response to PPD or Mtb stimulation. This observation suggests the presence of two populations *in vivo*, which may represent effector (antigen-independent *ex vivo* proliferation) and memory T cells (antigen-dependent *ex vivo* proliferation).[34] The antigen-independent (putative effector) $CD4^+$ and $CD8^+$ T cells were found at relatively high frequencies in the spleen during the first few weeks of CDC1551 infection and, thereafter, declined. The antigen-dependent T-cell population also peaked early and then declined, but a small pool of these cells appeared to persist after the clearance of cultivable bacilli from the lungs, consistent with a memory T-cell phenotype.[35] This interpretation, however, remains to be proved, because the immunological reagents necessary to define subsets of effector and memory T cells in the rabbit are not available. Despite the potential presence of abundant B cells in the lungs, B-cell activation, as determined by PPD-specific IgG production, was also minimal in CDC1551-infected rabbits, compared with levels seen in rabbits with progressive cavitary TB after HN878 infection.[30] However, because the reagent used to detect B cells was not rabbit B-cell specific, it is possible that the frequency of this cell population among the total lymphoid cells was overestimated. Taken together, our observations suggest that the magnitude of the acquired immune response during both LTBI and chronic active disease appears to track with the antigenic load.[36,37]

In most mouse strains, Mtb infection is chronic and the bacilli are not cleared from the lungs. Thus, the sustained T-cell activation in these animals, although essential to stabilize the bacillary load in the lungs, is not associated

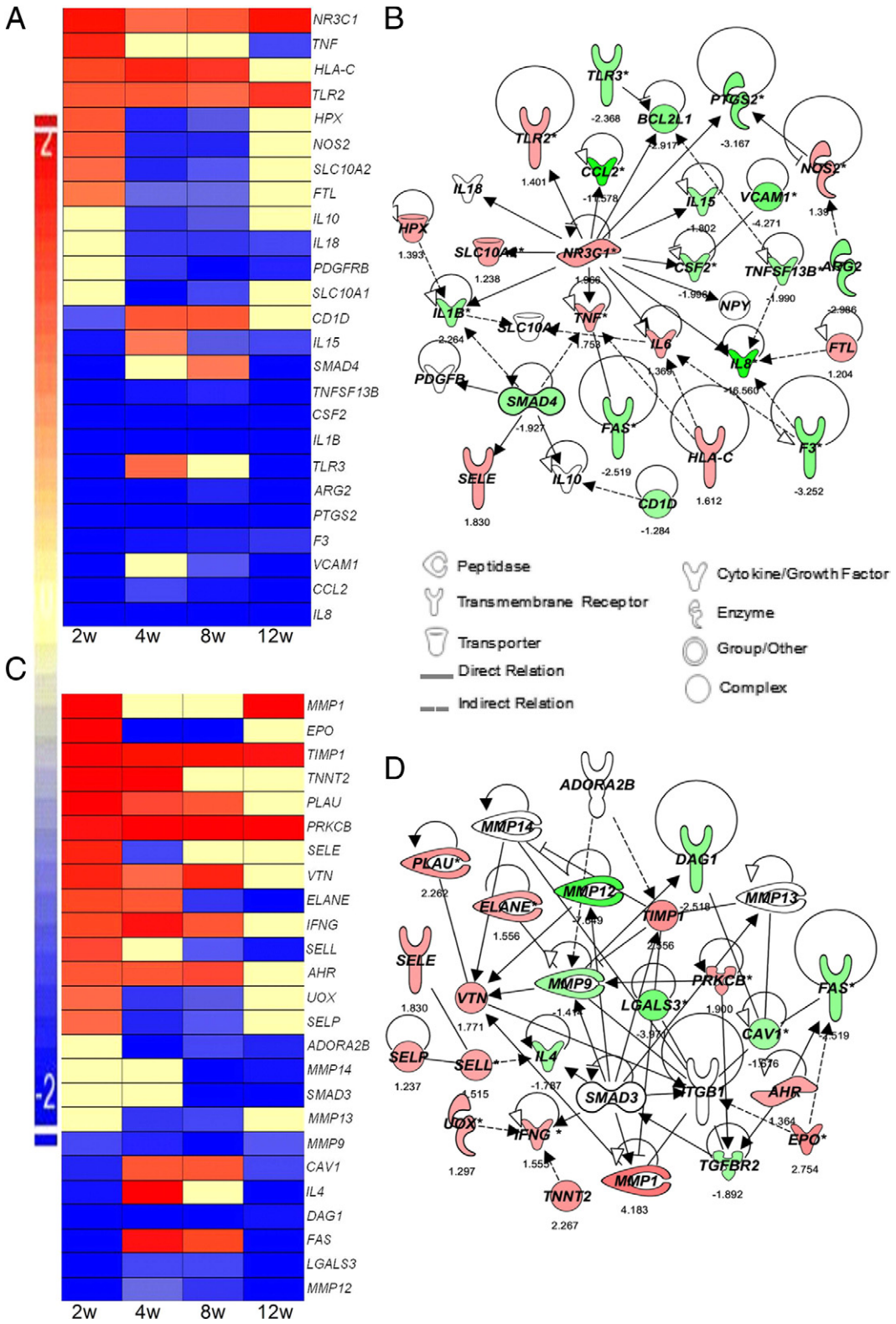

Figure 4. Differential expression of host genes involved in macrophage activation (**A** and **B**) and fibrosis/tissue remodeling (**C** and **D**) networks in *Mtb*-infected rabbit lungs. **A:** Intensity plot (heat map) of 25 significantly differentially expressed rabbit genes that constitute the macrophage activation network. The expression values were arranged in a descending manner (from top to bottom) at 2 weeks. **B:** Interaction map of member genes of the macrophage activation network at 2 weeks p.i. **C:** Heat map of significantly differentially expressed rabbit genes involved in fibrosis and the tissue remodeling network in the lungs. The expression values are sorted in a descending manner (from top to bottom) at 2 weeks. **D:** Interaction among the members of fibrosis and tissue remodeling network genes at 2 weeks p.i. For **A** and **C**, the color scale ranges from 2 (up-regulated; red) to −2 (down-regulated; blue), and yellow indicates the absence or insignificant expression of the gene. For **B** and **D**, green represents down-regulation; red, up-regulation; and no color, the absence or insignificant expression of the gene. Intensity in the colors of gene symbols corresponds to their respective level of expression as numerically mentioned under each gene symbol. Values presented are normalized to the level of expression observed in uninfected rabbit lungs.

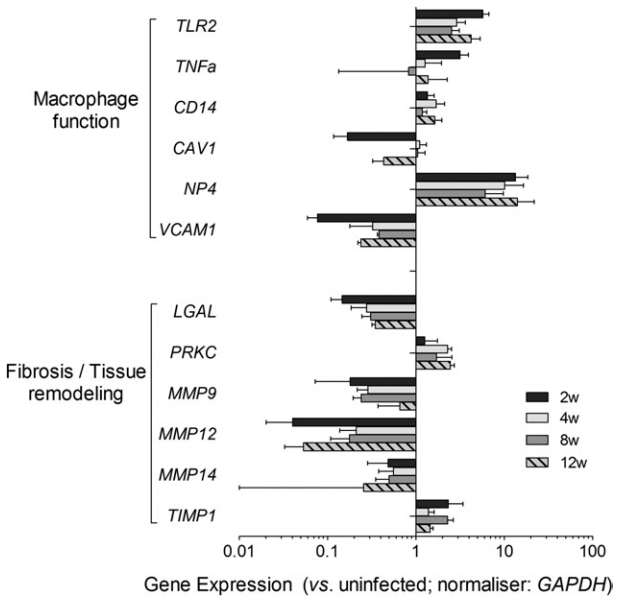

Figure 5. Quantification of selected differentially expressed genes involved in macrophage function and fibrosis/tissue remodeling during Mtb CDC1551 infection in rabbit lungs. The expression level of selected rabbit genes is quantified by real-time qPCR, normalized against the housekeeping gene *GAPDH*, and represented as relative fold compared with the expression levels in uninfected, naïve rabbits. The expression level of each gene plotted in the graph is median ± SE, measured in triplicate reactions from at least three different experiments. $P < 0.05$ compared to uninfected for all genes except *TNFa* and *CAV1* at 8w and *MMP14* at 12 weeks.

with complete clearance of the infection (ie, protection against TB). Rather, sustained T-cell activation is seen with adaptation of the host immune response to chronic antigenic stimulation.[35,38] Our observations in the rabbit LTBI model support a recently emerging idea that outcome of Mtb infection is largely determined by the kinetics of recruitment and activation of the lymphocytes in response to Mtb infection, rather than simply the overall numbers of T cells.[39–42] Indeed, although $CD4^+$ T-cell–deficient mice failed to control Mtb infection, later depletion of the $CD4^+$ T cells in the antibiotic-dependent mouse TB latency model (Cornell model) showed minimal impact on bacillary control.[43,44] In addition, during early infection of nonhuman primates, anti-mycobacterial immunity was dependent on the presence of $CD4^+$ T cells, whereas depletion of these cells in animals with LTBI had less impact on Mtb control.[45] In human studies, patients with TB who had chronic disease displayed progressive impairment of Mtb-specific T-cell responses with increasing bacillary loads. In these patients, a reduction in the relative numbers of polyfunctional $CD4^+$ T cells and increased frequencies of $CD8^+$ T cells, compared with individuals with LTBI, were seen.[36] Moreover, in bacille Calmette-Guérin–vaccinated neonates, we have shown that the frequency of cytokine-producing T cells, including both monofunctional and polyfunctional, does not predict protection against progression of Mtb infection to active disease.[46,47]

Macrophages play a central role in the host immune response to Mtb infection.[48,49] However, although optimal macrophage activation and TNF-α production are essential for controlling the growth and/or killing of intracellular Mtb, overproduction or chronically elevated levels of TNF-α can lead to exacerbated inflammation and tissue damage.[50,51] Indeed, in rabbits with chronic HN878 infection, in which macrophage activation and TNF-α production are sustained, extensive necrosis and lung tissue damage are seen.[30] In the rabbit model of LTBI, we observed an early activation of macrophages and increased *TNFα* transcript levels in the lungs of infected animals. This response was associated with the control of growth and clearance of the bacilli and dampened when the bacillary load was reduced. Consequently, in the absence of elevated *TNFα* levels, no necrosis was seen in the evolving lung granulomas. Moreover, once bacillary growth was controlled and the frequency of macrophages producing TNF-α in the tissues declined, the chronic mononuclear leukocyte inflammatory response, manifested as granulomas in the lungs, resolved. Consistent with this finding, the expression of the macrophage activation and inflammatory network genes, including *TNFα*, was up-regulated in the lungs during early infection and progressively declined as the infection was controlled. In contrast, the expression of *TLR2* was up-regulated and persisted until bacillary clearance was seen in the infected rabbit lungs. TLR2 is expressed on cells of both innate and adaptive immunity, plays a crucial role in the recognition and killing of virulent Mtb strains, and is essential to prevent progression of disease.[52,53] In the absence of TLR2, as seen in TLR2-deficient mice, uncontrolled lung bacillary growth, decreased immune cell migration, and a defective granulomatous response in the lungs were noted, resulting in exacerbated inflammation.[54,55] Thus, the persistence of elevated TLR2 in the CDC1551-infected rabbits may have been associated with the bacillary clearance and limited pathological characteristics seen in the lungs. In addition, we noted a significant down-regulation in the transcript levels of IL-1β, IL-8, and CCL2 in the Mtb-infected rabbit lungs. These results are consistent with reports describing elevated levels of these cytokines in the blood of patients with active TB, compared with uninfected and latently infected individuals.[56,57]

Chronic inflammation, such as seen during active pulmonary TB, can drive granuloma enlargement and caseation, cavity formation, and fibrosis, involving extensive fibroblast proliferation and collagen deposition around the granulomas in the infected organs.[29,58] Matrix metalloproteinases (MMPs), a family of proteases that includes collagenase, esterase, and stromelysins, play a key role in fibrosis, extracellular matrix destruction, and tissue remodeling during progressive TB.[58] More important, TNF-α, the most prominent inflammatory cytokine involved in TB pathogenesis, regulates the expression of several MMPs, and tissue inhibitor of MMP-1 (TIMP-1) is a negative regulator of MMP-9.[59,60] During CDC1551 infection, we observed the down-regulation of several important fibrosis network genes, including *MMP9*, *MMP12*, *MMP13*, and *MMP14*, with concomitant up-regulation of *TIMP1* expression, together with a lack of fibrosis in the lungs, as demonstrated by immunohistological analysis. These results are consistent with observations of higher

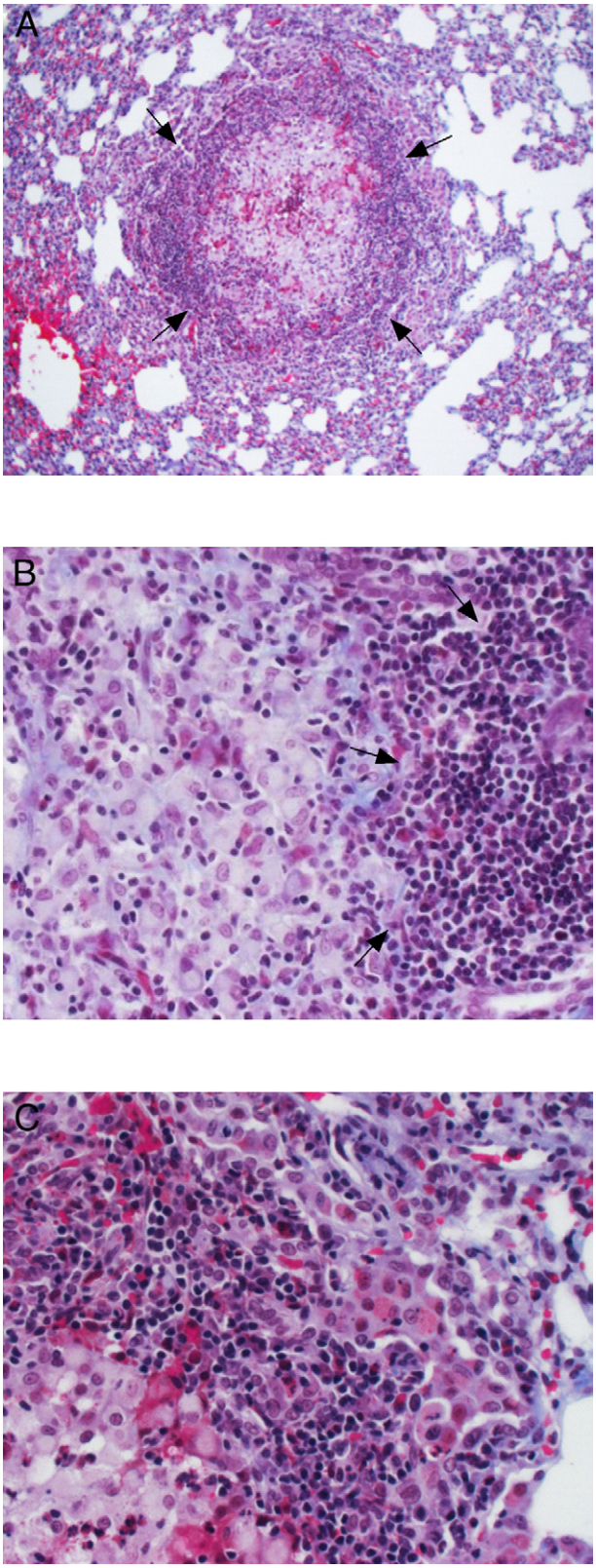

Figure 6. Extent of fibrosis in the Mtb CDC1551-infected rabbit lungs at 12 weeks p.i. **A–C:** The Gomori's trichrome-stained sections (collagen stains blue) show minimal fibrosis within and around the well-defined granuloma composed of central epithelioid macrophages and a peripheral lymphocyte cuff (**arrows** in **A** and **B**) in the infected rabbit lungs. This is in contrast to the highly fibrotic lesions seen when rabbits are infected for 12 to 16 weeks with Mtb HN878.[29] The images were photographed. Original magnification: ×10 (**A**); ×40 (**B** and **C**).

levels of MMP-9 in the serum of patients with active TB compared with uninfected individuals and the presence of abundant MMP-9 levels found in multinucleated giant cells surrounding the necrotic lesions of lymph node biopsy specimens from patients with active TB.[61,62] In our rabbit model, *SELE* and *SELP*, which encode the E- and L-selectin cell adhesion molecules, were moderately up-regulated at 2 weeks and gradually down-regulated at later times of infection, consistent with the absence of active, progressive pathological characteristics in these animals. In patients with active TB, levels of *SELE* and *SELP* were elevated compared with uninfected control subjects, and increased levels of serum E- and L-selectins directly correlated with the severity of disease, as determined by radiological diagnosis.[63]

Complete and spontaneous clearance of cultivable bacilli from the infected lung is considered a hallmark of LTBI in humans.[64,65] In the mouse and guinea pig models of Mtb infection, the bacteria are maintained at relatively high numbers in the infected lungs, whereas in the rat model, Mtb CFU numbers are reduced by the host immune response, but the bacilli are not fully cleared.[65,66] Anti-TB drug therapy must be administered to obtain full clearance of cultivable Mtb from the lungs of these animal species.[22,23] Even in the rabbit, not all Mtb strains are cleared spontaneously. Thus, the nature of the infecting Mtb strain significantly affects the host-pathogen interactions and determines the outcome of infection in these and other animal species.[14,67,68] Thus far, only Mtb CDC1551 infection of rabbits has consistently resulted in complete clearance of the bacilli from the lungs. Mtb HN878 infection was not controlled by the rabbit immune response.[30] Although Mtb H37Rv numbers in rabbits were reduced with time, the bacilli were not fully cleared, even after 20 weeks of pulmonary infection.[17,19,20,69,70] Multiple studies have focused on identifying the *Mtb* genes and their products that determine whether the bacilli can subvert the host immune response and continue growing, or whether they are controlled and cleared.[71,72] Prominent among the putative Mtb strain-specific determinants are several lipids, which appear to have immune-modulatory capabilities, suggesting that such capacity may be an important feature of the success of this pathogen in human populations.[73–75] Ultimately, an understanding of the host and pathogen factors that determine the outcome after Mtb infection, whether individuals develop active infectious TB or LTBI, will facilitate the development of better intervention for improved TB control.

Acknowledgments

We thank Dr. Claudia Manca for useful discussions, Sabrina F. Dalton for assistance with manuscript preparation, and the staff of the Center for Applied Genomics of the Public Health Research Institute for the microarray experiments.

References

1. WHO: Global Tuberculosis Control Report. Geneva, Switzerland, World Health Organization, 2011
2. Lonnroth K, Jaramillo E, Williams BG, Dye C, Raviglione M: Drivers of tuberculosis epidemics: the role of risk factors and social determinants. Soc Sci Med 2009, 68:2240–2246
3. Mack U, Migliori GB, Sester M, Rieder HL, Ehlers S, Goletti D, Bossink A, Magdorf K, Holscher C, Kampmann B, Arend SM, Detjen A, Bothamley G, Zellweger JP, Milburn H, Diel R, Ravn P, Cobelens F, Cardona PJ, Kan B, Solovic I, Duarte R, Cirillo DM: LTBI: latent tuberculosis infection or lasting immune responses to M. tuberculosis? a TBNET consensus statement. Eur Respir J 2009, 33:956–973
4. Feldman WH, Baggenstoss AH: The occurrence of virulent tubercle bacilli in presumably non-tuberculous lung tissue. Am J Pathol 1939, 15:501–515
5. Barry CE 3rd, Boshoff HI, Dartois V, Dick T, Ehrt S, Flynn J, Schnappinger D, Wilkinson RJ, Young D: The spectrum of latent tuberculosis: rethinking the biology and intervention strategies. Nat Rev Microbiol 2009, 7:845–855
6. Achkar JM, Jenny-Avital ER: Incipient and subclinical tuberculosis: defining early disease states in the context of host immune response. J Infect Dis 2011, 204(Suppl 4):S1179–S1186
7. Lin PL, Flynn JL: Understanding latent tuberculosis: a moving target. J Immunol 2010, 185:15–22
8. Bellamy R, Ruwende C, Corrah T, McAdam KP, Whittle HC, Hill AV: Variations in the NRAMP1 gene and susceptibility to tuberculosis in West Africans. N Engl J Med 1998, 338:640–644
9. Thye T, Owusu-Dabo E, Vannberg FO, van Crevel R, Curtis J, Sahiratmadja E, Balabanova Y, Ehmen C, Muntau B, Ruge G, Sievertsen J, Gyapong J, Nikolayevskyy V, Hill PC, Sirugo G, Drobniewski F, van de Vosse E, Newport M, Alisjahbana B, Nejentsev S, Ottenhoff TH, Hill AV, Horstmann RD, Meyer CG: Common variants at 11p13 are associated with susceptibility to tuberculosis. Nat Genet 2012, 44:257–259
10. Baker AR, Zalwango S, Malone LL, Igo RP Jr, Qiu F, Nsereko M, Adams MD, Supelak P, Mayanja-Kizza H, Boom WH, Stein CM: Genetic susceptibility to tuberculosis associated with cathepsin Z haplotype in a Ugandan household contact study. Hum Immunol 2011, 72:426–430
11. Hijikata M, Shojima J, Matsushita I, Tokunaga K, Ohashi J, Hang NT, Horie T, Sakurada S, Hoang NP, Thuong PH, Lien LT, Keicho N: Association of IFNGR2 gene polymorphisms with pulmonary tuberculosis among the Vietnamese. Hum Genet 2012, 131:675–682
12. Homolka S, Niemann S, Russell DG, Rohde KH: Functional genetic diversity among Mycobacterium tuberculosis complex clinical isolates: delineation of conserved core and lineage-specific transcriptomes during intracellular survival. PLoS Pathog 2010, 6:e1000988
13. Palanisamy GS, DuTeau N, Eisenach KD, Cave DM, Theus SA, Kreiswirth BN, Basaraba RJ, Orme IM: Clinical strains of Mycobacterium tuberculosis display a wide range of virulence in guinea pigs. Tuberculosis (Edinb) 2009, 89:203–209
14. Krishnan N, Malaga W, Constant P, Caws M, Tran TH, Salmons J, Nguyen TN, Nguyen DB, Daffe M, Young DB, Robertson BD, Guilhot C, Thwaites GE: Mycobacterium tuberculosis lineage influences innate immune response and virulence and is associated with distinct cell envelope lipid profiles. PLoS One 2011, 6:e23870
15. Manca C, Reed MB, Freeman S, Mathema B, Kreiswirth B, Barry CE 3rd, Kaplan G: Differential monocyte activation underlies strain-specific Mycobacterium tuberculosis pathogenesis. Infect Immun 2004, 72:5511–5514
16. Manca C, Tsenova L, Barry CE 3rd, Bergtold A, Freeman S, Haslett PA, Musser JM, Freedman VH, Kaplan G: Mycobacterium tuberculosis CDC1551 induces a more vigorous host response in vivo and in vitro, but is not more virulent than other clinical isolates. J Immunol 1999, 162:6740–6746
17. Flynn J, Tsenova L, Izzo A, Kaplan G: Experimental Animal Models of Tuberculosis. Edited by Britton, WJ. Weinheim, Germany, Wiley-VCH Verlag, 2008, pp 389–426
18. Manabe YC, Dannenberg AM Jr, Tyagi SK, Hatem CL, Yoder M, Woolwine SC, Zook BC, Pitt ML, Bishai WR: Different strains of Mycobacterium tuberculosis cause various spectrums of disease in the rabbit model of tuberculosis. Infect Immun 2003, 71:6004–6011
19. Bishai WR, Dannenberg AM Jr, Parrish N, Ruiz R, Chen P, Zook BC, Johnson W, Boles JW, Pitt ML: Virulence of Mycobacterium tuberculosis CDC1551 and H37Rv in rabbits evaluated by Lurie's pulmonary tubercle count method. Infect Immun 1999, 67:4931–4934
20. Tsenova L, Ellison E, Harbacheuski R, Moreira AL, Kurepina N, Reed MB, Mathema B, Barry CE 3rd, Kaplan G: Virulence of selected Mycobacterium tuberculosis clinical isolates in the rabbit model of meningitis is dependent on phenolic glycolipid produced by the bacilli. J Infect Dis 2005, 192:98–106
21. Kaplan G, Tsenova L: Pulmonary tuberculosis in the rabbit. A Color Atlas of Comparative Pathology of Pulmonary Tuberculosis. Edited by Leong, FJ Dartois, V Dick, T. Singapore, CRC Press, Taylor & Francis Group, 2010, pp 107–129
22. Gupta UD, Katoch VM: Animal models of tuberculosis. Tuberculosis (Edinb) 2005, 85:277–293
23. Shi C, Shi J, Xu Z: A review of murine models of latent tuberculosis infection. Scand J Infect Dis 2011, 43:848–856
24. Chao MC, Rubin EJ: Letting sleeping dos lie: does dormancy play a role in tuberculosis? Annu Rev Microbiol 2010, 64:293–311
25. Capuano SV 3rd, Croix DA, Pawar S, Zinovik A, Myers A, Lin PL, Bissel S, Fuhrman C, Klein E, Flynn JL: Experimental Mycobacterium tuberculosis infection of cynomolgus macaques closely resembles the various manifestations of human M. tuberculosis infection. Infect Immun 2003, 71:5831–5844
26. Lin PL, Rodgers M, Smith L, Bigbee M, Myers A, Bigbee C, Chiosea I, Capuano SV, Fuhrman C, Klein E, Flynn JL: Quantitative comparison of active and latent tuberculosis in the cynomolgus macaque model. Infect Immun 2009, 77:4631–4642
27. Parrish NM, Dick JD, Bishai WR: Mechanisms of latency in Mycobacterium tuberculosis. Trends Microbiol 1998, 6:107–112
28. Koo MS, Subbian S, Kaplan G: Strain specific transcriptional response in Mycobacterium tuberculosis infected macrophages. Cell Commun Signal 2012, 10:2
29. Subbian S, Tsenova L, O'Brien P, Yang G, Koo MS, Peixoto B, Fallows D, Zeldis JB, Muller G, Kaplan G: Phosphodiesterase-4 inhibition combined with isoniazid treatment of rabbits with pulmonary tuberculosis reduces macrophage activation and lung pathology. Am J Pathol 2011, 179:289–301
30. Subbian S, Tsenova L, Yang G, O'Brien P, Parsons S, Peixoto B, Taylor L, Fallows D, Kaplan G: Chronic pulmonary cavitary tuberculosis in rabbits: a failed host immune response. Open Biol 2011, 1:110016
31. Subbian S, Tsenova L, O'Brien P, Yang G, Koo MS, Peixoto B, Fallows D, Dartois V, Muller G, Kaplan G: Phosphodiesterase-4 inhibition alters gene expression and improves isoniazid-mediated clearance of Mycobacterium tuberculosis in rabbit lungs. PLoS Pathog 2011, 7:e1002262
32. Subbian S, Mehta PK, Cirillo SL, Cirillo JD: The Mycobacterium marinum mel2 locus displays similarity to bacterial bioluminescence systems and plays a role in defense against reactive oxygen and nitrogen species. BMC Microbiol 2007, 7:4
33. Chan J, Flynn J: The immunological aspects of latency in tuberculosis. Clin Immunol 2004, 110:2–12
34. Gideon HP, Flynn JL: Latent tuberculosis: what the host "sees"? Immunol Res 2011, 50:202–212
35. Lanzavecchia A, Sallusto F: Understanding the generation and function of memory T cell subsets. Curr Opin Immunol 2005, 17:326–332
36. Day CL, Abrahams DA, Lerumo L, Janse van Rensburg E, Stone L, O'Rie T, Pienaar B, de Kock M, Kaplan G, Mahomed H, Dheda K, Hanekom WA: Functional capacity of Mycobacterium tuberculosis-specific T cell responses in humans is associated with mycobacterial load. J Immunol 2011, 187:2222–2232
37. Wolf AJ, Desvignes L, Linas B, Banaiee N, Tamura T, Takatsu K, Ernst JD: Initiation of the adaptive immune response to Mycobacterium tuberculosis depends on antigen production in the local lymph node, not the lungs. J Exp Med 2008, 205:105–115
38. van Pinxteren LA, Cassidy JP, Smedegaard BH, Agger EM, Andersen P: Control of latent Mycobacterium tuberculosis infection is dependent on CD8 T cells. Eur J Immunol 2000, 30:3689–3698
39. Urdahl KB, Shafiani S, Ernst JD: Initiation and regulation of T-cell responses in tuberculosis. Mucosal Immunol 2011, 4:288–293
40. Reiley WW, Shafiani S, Wittmer ST, Tucker-Heard G, Moon JJ, Jenkins MK, Urdahl KB, Winslow GM, Woodland DL: Distinct functions of

antigen-specific CD4 T cells during murine Mycobacterium tuberculosis infection. Proc Natl Acad Sci U S A 2010, 107:19408–19413
41. Ulrichs T, Kosmiadi GA, Jorg S, Pradl L, Titukhina M, Mishenko V, Gushina N, Kaufmann SH: Differential organization of the local immune response in patients with active cavitary tuberculosis or with nonprogressive tuberculoma. J Infect Dis 2005, 192:89–97
42. Brighenti S, Andersson J: Local immune responses in human tuberculosis: learning from the site of infection. J Infect Dis 2012, 205(Suppl 2):S316–S324
43. Caruso AM, Serbina N, Klein E, Triebold K, Bloom BR, Flynn JL: Mice deficient in CD4 T cells have only transiently diminished levels of IFN-gamma, yet succumb to tuberculosis. J Immunol 1999, 162: 5407–5416
44. Scanga CA, Mohan VP, Joseph H, Yu K, Chan J, Flynn JL: Reactivation of latent tuberculosis: variations on the Cornell murine model. Infect Immun 1999, 67:4531–4538
45. Lin PL, Rutledge T, Green AM, Bigbee M, Fuhrman C, Klein E, Flynn JL: CD4 T cell depletion exacerbates acute Mycobacterium tuberculosis while reactivation of latent infection is dependent on severity of tissue depletion in cynomolgus macaques. AIDS Res Hum Retroviruses 2012, doi:10.1089/aid.2012.0028. [Epub ahead of press]
46. Hanekom WA, Abel B, Scriba TJ: Immunological protection against tuberculosis. S Afr Med J 2007, 97:973–977
47. Kagina BM, Abel B, Scriba TJ, Hughes EJ, Keyser A, Soares A, Gamieldien H, Sidibana M, Hatherill M, Gelderbloem S, Mahomed H, Hawkridge A, Hussey G, Kaplan G, Hanekom WA: Specific T cell frequency and cytokine expression profile do not correlate with protection against tuberculosis after bacillus Calmette-Guerin vaccination of newborns. Am J Respir Crit Care Med 2010, 182:1073–1079
48. Flynn JL, Chan J, Lin PL: Macrophages and control of granulomatous inflammation in tuberculosis. Mucosal Immunol 2011, 4:271–278
49. Gordon S, Martinez FO: Alternative activation of macrophages: mechanism and functions. Immunity 2010, 32:593–604
50. Bekker LG, Moreira AL, Bergtold A, Freeman S, Ryffel B, Kaplan G: Immunopathologic effects of tumor necrosis factor alpha in murine mycobacterial infection are dose dependent. Infect Immun 2000, 68:6954–6961
51. Quesniaux VF, Jacobs M, Allie N, Grivennikov S, Nedospasov SA, Garcia I, Olleros ML, Shebzukhov Y, Kuprash D, Vasseur V, Rose S, Court N, Vacher R, Ryffel B: TNF in host resistance to tuberculosis infection. Curr Dir Autoimmun 2010, 11:157–179
52. Jo EK, Yang CS, Choi CH, Harding CV: Intracellular signalling cascades regulating innate immune responses to Mycobacteria: branching out from Toll-like receptors. Cell Microbiol 2007, 9:1087–1098
53. Yoshida A, Inagawa H, Kohchi C, Nishizawa T, Soma G: The role of toll-like receptor 2 in survival strategies of Mycobacterium tuberculosis in macrophage phagosomes. Anticancer Res 2009, 29:907–910
54. Drennan MB, Nicolle D, Quesniaux VJ, Jacobs M, Allie N, Mpagi J, Fremond C, Wagner H, Kirschning C, Ryffel B: Toll-like receptor 2-deficient mice succumb to Mycobacterium tuberculosis infection. Am J Pathol 2004, 164:49–57
55. Tjarnlund A, Guirado E, Julian E, Cardona PJ, Fernandez C: Determinant role for Toll-like receptor signalling in acute mycobacterial infection in the respiratory tract. Microbes Infect 2006, 8:1790–1800
56. Frahm M, Goswami ND, Owzar K, Hecker E, Mosher A, Cadogan E, Nahid P, Ferrari G, Stout JE: Discriminating between latent and active tuberculosis with multiple biomarker responses. Tuberculosis (Edinb) 2011, 91:250–256
57. Wu B, Huang C, Kato-Maeda M, Hopewell PC, Daley CL, Krensky AM, Clayberger C: Messenger RNA expression of IL-8, FOXP3, and IL-12beta differentiates latent tuberculosis infection from disease. J Immunol 2007, 178:3688–3694
58. Elkington PT, Ugarte-Gil CA, Friedland JS: Matrix metalloproteinases in tuberculosis. Eur Respir J 2011, 38:456–464
59. Elkington PT, D'Armiento JM, Friedland JS: Tuberculosis immunopathology: the neglected role of extracellular matrix destruction. Sci Transl Med 2011, 3:71ps76
60. Elass E, Aubry L, Masson M, Denys A, Guerardel Y, Maes E, Legrand D, Mazurier J, Kremer L: Mycobacterial lipomannan induces matrix metalloproteinase-9 expression in human macrophagic cells through a Toll-like receptor 1 (TLR1)/TLR2- and CD14-dependent mechanism. Infect Immun 2005, 73:7064–7068
61. El-Masry S, Lotfy M, Samy M, Moawia S, El-Sayed IH, Khamees IM: Pattern of matrix metalloproteinases-9, P53 and BCL-2 proteins in Egyptian patients with pulmonary Mycobacterium tuberculosis. Acta Microbiol Immunol Hung 2010, 57:123–133
62. Zhu XW, Price NM, Gilman RH, Recarvarren S, Friedland JS: Multinucleate giant cells release functionally unopposed matrix metalloproteinase-9 in vitro and in vivo. J Infect Dis 2007, 196:1076–1079
63. Mukae H, Ashitani J, Tokojima M, Ihi T, Kohno S, Matsukura S: Elevated levels of circulating adhesion molecules in patients with active pulmonary tuberculosis. Respirology 2003, 8:326–331
64. Ehlers S: Lazy, dynamic or minimally recrudescent? on the elusive nature and location of the mycobacterium responsible for latent tuberculosis. Infection 2009, 37:87–95
65. Riska PF, Carleton S: Latent tuberculosis: models, mechanisms, and novel prospects for eradication. Semin Pediatr Infect Dis 2002, 13: 263–272
66. Singhal A, Aliouat el M, Herve M, Mathys V, Kiass M, Creusy C, Delaire B, Tsenova L, Fleurisse L, Bertout J, Camacho L, Foo D, Tay HC, Siew JY, Boukhouchi W, Romano M, Mathema B, Dartois V, Kaplan G, Bifani P: Experimental tuberculosis in the Wistar rat: a model for protective immunity and control of infection. PLoS One 2011, 6:e18632
67. Marquina-Castillo B, Garcia-Garcia L, Ponce-de-Leon A, Jimenez-Corona ME, Bobadilla-Del Valle M, Cano-Arellano B, Canizales-Quintero S, Martinez-Gamboa A, Kato-Maeda M, Robertson B, Young D, Small P, Schoolnik G, Sifuentes-Osornio J, Hernandez-Pando R: Virulence, immunopathology and transmissibility of selected strains of Mycobacterium tuberculosis in a murine model. Immunology 2009, 128:123–133
68. Be NA, Klinkenberg LG, Bishai WR, Karakousis PC, Jain SK: Strain-dependent CNS dissemination in guinea pigs after Mycobacterium tuberculosis aerosol challenge. Tuberculosis (Edinb) 2011, 91:386–389
69. Barczak AK, Domenech P, Boshoff HI, Reed MB, Manca C, Kaplan G, Barry CE 3rd: In vivo phenotypic dominance in mouse mixed infections with Mycobacterium tuberculosis clinical isolates. J Infect Dis 2005, 192:600–606
70. Kesavan AK, Brooks M, Tufariello J, Chan J, Manabe YC: Tuberculosis genes expressed during persistence and reactivation in the resistant rabbit model. Tuberculosis (Edinb) 2009, 89:17–21
71. Paige C, Bishai WR: Penitentiary or penthouse condo: the tuberculous granuloma from the microbe's point of view. Cell Microbiol 2010, 12:301–309
72. Saunders BM, Britton WJ: Life and death in the granuloma: immunopathology of tuberculosis. Immunol Cell Biol 2007, 85:103–111
73. Rindi L, Peroni I, Lari N, Bonanni D, Tortoli E, Garzelli C: Variation of the expression of Mycobacterium tuberculosis ppe44 gene among clinical isolates. FEMS Immunol Med Microbiol 2007, 51:381–387
74. Reed MB, Domenech P, Manca C, Su H, Barczak AK, Kreiswirth BN, Kaplan G, Barry CE 3rd: A glycolipid of hypervirulent tuberculosis strains that inhibits the innate immune response. Nature 2004, 431:84–87
75. Flores J, Espitia C: Differential expression of PE and PE_PGRS genes in Mycobacterium tuberculosis strains. Gene 2003, 318:75–81